

# A Concordant “Freely Coasting” Cosmology

Savita Gehlaut, Pranav Kumar

Geetanjali and Daksh Lohiya\*

*Department of Physics and Astrophysics,  
University of Delhi, Delhi-110007, India*

ℰ

*Inter University Centre for Astronomy and Astrophysics  
Ganeskhind, Pune 411 007, India*

## Abstract

A strictly linear evolution of the cosmological scale factor is surprisingly an excellent fit to a host of cosmological observations. Any model that can support such a coasting presents itself as a falsifiable model as far as classical cosmological tests are concerned. Such evolution is known to be comfortably concordant with the Hubble diagram as deduced from data of recent supernovae 1a and high redshift objects, it passes constraints arising from the age and gravitational lensing statistics and clears basic constraints on nucleosynthesis. Such an evolution exhibits distinguishable and verifiable features for the recombination era. This article discusses the concordance of such an evolution in relation to minimal requirements for large scale structure formation and cosmic microwave background anisotropy along with the overall viability of such models.

While these results should be of interest for a host of alternative gravity models that support a linear coasting, we conjecture that a linear evolution would emerge naturally either from General Relativity itself or from a General Relativistic theory of a non-minimally coupled scalar field theory.

---

\*E-mail : dlohiya@iucaa.ernet.in

# 1 Introduction

Large scale homogeneity and isotropy observed in the universe implies the Friedman-Robertson-Walker (FRW) metric:

$$ds^2 = dt^2 - a(t)^2 \left[ \frac{dr^2}{1 - Kr^2} + r^2(d\theta^2 + \sin^2\theta d\phi^2) \right] \quad (1)$$

Here  $K = \pm 1, 0$  is the curvature constant. In standard “big-bang” cosmology, the scale factor  $a(t)$  is determined by the equation of state of matter and Einstein’s equations. The scale factor, in turn, determines the response of a chosen model to cosmological observations. Four decades ago, the main “classical” cosmological tests were (1) The galaxy number count as a function of redshift; (2) The angular diameter of “standard” objects (galaxies) as a function of redshift; and finally (3) The apparent luminosity of a “standard candle” as a function of redshift. Over the last two decades, other tests that standard cosmology has been subjected to are: the early universe nucleosynthesis constraints, estimates of age of the universe in comparison to ages of old objects, statistics of gravitational lensing, constraints from large scale structure formation and finally, the physics of recombination as deduced from cosmic microwave background anisotropy.

In this article we explore concordance of the above observations with a FRW cosmology in which the scale factor evolves linearly with time:  $a(t) \propto t$ , right from the creation event itself. The motivation for such an endeavor has been discussed at length in a series of earlier articles [1]. First of all, the use of Einstein’s equations to describe cosmology has never ever been justified. The averaging problem and the continuum limit in General Relativity have not been properly addressed. In any case, most treatments have not considered the retarded effects in their full generality[2, 3, 4]. Averaging Einsteins equations across horizon lengths lacks self consistency. On the other hand, Newtonian cosmology, applied to an exploding *Milne ball* in a flat space-time [see eg. [5, 6]] gives a unique linear coasting cosmology viz. the FRW [*Milne*] metric with  $a(t) = t$ . Such a cosmology does not suffer from the horizon problem. As a matter of fact, a linearly evolving model is the only power law model that has neither a particle horizon nor a cosmological event horizon. Linear evolution is also purged of the flatness or the fine tuning problem

[1, 7, 9]. The scale factor in such theories does not constrain the matter density parameter. The Linear coasting characteristic of a Newtonian cosmology can be dynamically generated. As a matter of fact, it is a generic feature in a class of models that attempt to dynamically solve the cosmological constant problem [8, 7, 9, 10, 11]. Particularly appealing in a fourth order conformally invariant model of Mannheim and Kazanas [11]. Gravitation is determined by a fourth order (Weyl tensor squared) action that identically vanishes for the conformally flat FRW metric. A non-minimally coupled scalar field then produces an effective *repulsive gravitation* that quickly constrains the universe to a linear coasting. Non-conformally flat perturbations around this linear coasting background can be effectively described by eqn(3) below.

We may take any of the above as the basis for our linear coasting conjecture. In what follows, we assume that an homogeneous background FRW universe is born and evolves as a Milne Universe about which a matter distribution and standard General Relativity would determine the growth of perturbations. The following sections describe standard aspects of cosmology that follows.

## 2 A linearly coasting cosmology

### 2.1 Classical Cosmology tests

Kolb[12] was probably first to demonstrate that data on Galaxy number counts as a function of red-shift as well as data on angular diameter distance as a function of red-shift do not rule out a linearly coasting cosmology. Unfortunately, these two tests are marred by effects such as galaxy mergers and galactic evolution. For these reasons these tests have fallen into disfavour as reliable indicators of a viable model.

The variation of apparent luminosity of a “standard candle” as a function of red-shift is referred to as the Hubble test. With the discovery of Supernovae type Ia [SNe Ia] as reliable standard candles, the status of Hubble test has been elevated to that of a precision measurement. Recent measurements by the supernovae cosmology project [13] eliminated the “minimal inflationary”

prediction defined by  $\Omega_\Lambda = 0$  and  $\Omega_M = 1$ . The data has been used to assess a “non-minimal inflationary cosmology” defined by  $\Omega_\Lambda \neq 0$ ,  $\Omega_\Lambda + \Omega_M = 1$ . The maximum likelihood analysis following from such a study has yielded the values  $\Omega_M = 0.28 \pm 0.1$  and  $\Omega_\Lambda = 0.72 \pm 0.1$  [13, 14, 15].

For a general power law cosmology with the scale factor  $a(t) = \bar{k}t^\alpha$ , with  $\bar{k}$ ,  $\alpha$  arbitrary constants, it is straightforward to discover the following relation between the apparent magnitude  $m(z)$ , the absolute magnitude  $M$  and the red-shift  $z$  of an object:

$$m(z) = \mathcal{M} + 5\log H_o + 5\log\left(\frac{\alpha}{H_o}\right)^\alpha (1+z)\bar{k}S\left[\frac{1}{(1-\alpha)\bar{k}}\left(\frac{\alpha}{H_o}\right)^{1-\alpha}(1-(1+z)^{1-\frac{1}{\alpha}})\right] \quad (2)$$

Here  $S[X] = X, \sin(X)$  or  $\sinh(X)$  for  $K = 0, \pm 1$  respectively, and  $\mathcal{M} = M - 5\log(H_o) + 25$ . The best fit turns out to be  $\alpha = 1.001 \pm .0043$ ,  $K = -1$ . [1]. The minimum  $\chi^2$  per degree of freedom turns out to be 1.18. This is comparable to the corresponding value 1.17 reported by Perlmutter et al for the constrained non-minimal inflationary cosmology. Linear coasting is as accommodating for more recent high red-shift objects as the standard non-minimal inflationary model. The concordance of linear coasting with SNeIa data finds a passing mention in the analysis of Perlmutter [13] who noted that the curve for  $\Omega_\Lambda = \Omega_M = 0$  (for which the scale factor would have a linear evolution) is “practically identical to **bestfit** plot for an unconstrained cosmology”. We display this “practical coincidence” in figure I that includes the more recent high redshift objects.

The age estimate of the ( $a(t) \propto t$ ) universe, deduced from a measurement of the Hubble parameter, is given by  $t_o = (H_o)^{-1}$ . The low red-shift SNeIa data [16, 17] gives the best value of 65 km sec<sup>-1</sup> Mpc<sup>-1</sup> for the Hubble parameter. The age of the universe turns out to be  $15 \times 10^9$  years. This is  $\approx 50\%$  greater than the age inferred from the same measurement in standard (cold) dark matter dominated cosmology (without the cosmological constant). Such an age estimate is comfortably concordant with age estimates of old clusters.

A study of consistency of linear coasting with gravitational lensing statistics has recently been reported [1]. The expected frequency of multiple image lensing events probes the viability of a given cosmology. A sample of 867 high luminosity optical quasars projected in a power law FRW cosmology gives an expected number of five lensed quasars for a linear coasting cosmology. This

indeed matches observations. Thus a strictly linear evolution of the scale factor is comfortably concordant with gravitational lensing statistics.

## 2.2 “The precision” tests

**a) The Nucleosynthesis Constraint** What makes linear coasting particularly appealing is a recent demonstration of primordial nucleosynthesis not to be an impediment for a linear coasting cosmology [1, 18]. A linear evolution of the scale factor may be expected to radically effect nucleosynthesis in the early universe. Surprisingly, the following scenario goes through.

Energy conservation, in a period where the baryon entropy ratio does not change, enables the distribution of photons to be described by an effective temperature  $T$  that scales as  $a(t)T = \text{constant}$ . With the age of the universe estimated from the Hubble parameter being  $\approx 1.5 \times 10^{10}$  years, and  $T_0 \approx 2.7K$ , one concludes that the age of the universe at  $T \approx 10^{10}K$  would be some four years [rather than a few seconds as in standard cosmology]. The universe would take some  $10^3$  years to cool to  $10^7K$ . With such time periods being large in comparison to the free neutron life time, one would hardly expect any neutrons to survive at temperatures relevant for nucleosynthesis. However, with such a low rate of expansion, weak interactions remain in equilibrium for temperatures as low as  $\approx 10^8K$ . The neutron - proton ratio keeps falling as  $n/p \approx \exp[-15/T_9]$ . Here  $T_9$  is the temperature in units of  $10^9K$  and the factor of 15 comes from the n-p mass difference in these units. There would again hardly be any neutrons left if nucleosynthesis were to commence at (say)  $T_9 \approx 1$ . However, as weak interactions are still in equilibrium, once nucleosynthesis commences, inverse beta decay would replenish neutrons by converting protons into neutrons and pumping them into the nucleosynthesis channel. With beta decay in equilibrium, the baryon entropy ratio determines a low enough nucleosynthesis rate that can remove neutrons out of the equilibrium buffer at a rate smaller than the relaxation time of the buffer. This ensures that neutron value remains unchanged as heavier nuclei build up. It turns out that for baryon entropy ratio  $\eta \approx 5 \times 10^{-9}$ , there would just be enough neutrons produced, after nucleosynthesis commences, to give  $\approx 23.9\%$  Helium and metallicity some  $10^8$  times the metallicity produced in the early universe in the standard scenario. This

metallicity is of the same order of magnitude as seen in lowest metallicity objects.

The only problem that one has to contend with is the significantly low yields of deuterium in such a cosmology. Though deuterium can be produced by spallation processes later in the history of the universe, it is difficult to produce the right amount without a simultaneous over production of Lithium [19]. However, as pointed out in [1], the amount of Helium produced is quite sensitive to  $\eta$  in such models. In an inhomogeneous universe, therefore, one can have the helium to hydrogen ratio to have a large primordial variation. Deuterium can be produced by a spallation process much later in the history of the universe. If one considers spallation of a helium deficient cloud onto a helium rich cloud, it is easy to produce deuterium as demonstrated by Epstein [19] - without overproduction of Lithium.

Interestingly, the baryon entropy ratio required for the right amount of helium corresponds to  $\Omega_b \approx 0.2$ . Here  $\Omega_b$  is the ratio of the baryon density to a “density parameter” determined by the Hubble constant:  $\Omega_b \equiv \rho_b/\rho_c = 8\pi G\rho_b/3H_0^2$ .  $\Omega_b \approx 0.2$  closes dynamic mass estimates of large galaxies and clusters [see eg [20, 21]]. In standard cosmology this closure is sought to be achieved by taking recourse to non-baryonic cold dark matter. Thus in a linearly scaling cosmology, there would be no need of non-baryonic cold dark matter to account for large scale galactic flows.

### **b) Density Perturbations**

We conjecture that the universe starts with a homogeneous isotropic distribution (eg. a Milne ball) and that an appropriate averaging procedure that correctly takes care of retarded effects in a relativistic gravity theory that accounts for a creation event, would support the large scale linear coasting with the metric described by eqn(1) with  $K = -1$ . Perturbations around this background shall be assumed to be described by

$$-8\pi G\delta T_{\mu\nu}^M = \delta G_{\mu\nu} \tag{3}$$

with  $\delta G_{\mu\nu}$  determined by perturbations around eqn(1). It would be fair to call this conjecture as a “Newtonian Cosmology conjecture” as Newton felt that one could justify the cancellation of gravity in a homogeneous and isotropic universe. Bertschinger [22] and Gibbons [23] have shown how consistent cosmological dynamics, indistinguishable from dynamics in the standard model,

follows from a Newtonian proposal in comoving rather than Minkowskian coordinates. In effect this amounts to stating that *a Homogeneous and isotropic universe with an arbitrary equation of state can be described by eqn(1), with  $a(t) = t$ ,  $K = -1$  and that perturbations around it are determined by eqn(3).* This further amounts to rejecting the unjustified assumptions of continuum limit (fluid approximation) and averaging that are usually taken for granted. Standard Einstein equations may well hold at the microscopic level but not as global averaged equations in a universe with a definite creation event. Further, as stated in the introduction, there are alternative gravity models that justify the above conjecture. In this article we have restricted ourselves to the consequences of such a conjecture.

To explore whether such small perturbations in the above model can evolve to give structures at large scales, we express the metric as

$$ds^2 = {}^{(o)}g_{\mu\nu}dx^\mu dx^\nu + \delta g_{\mu\nu}dx^\mu dx^\nu \quad (4)$$

with the background metric  ${}^{(o)}g_{\mu\nu}$  expressed in comoving coordinates as:

$${}^{(o)}g_{\mu\nu}dx^\mu dx^\nu = dt^2 - a(t)^2 \gamma_{ij} dx^i dx^j = a^2(\eta)(d\eta^2 - \gamma_{ij} dx^i dx^j) \quad (5)$$

$\eta$  is the conformal time ( $d\eta = a^{-1}dt$ ,  $a = t = t_0 e^\eta$ ), and

$$\gamma_{ij} = \delta_{ij} [1 - \frac{1}{4}(x^2 + y^2 + z^2)]^{-2} \quad (6)$$

The  $\delta g_{\mu\nu}$  describe the perturbation. These can be decomposed into scalar, vector or tensor type, depending on the way they transform on a constant  $\eta$  hypersurface. In the following, we consider scalar perturbations only. Following standard arguments, vector perturbations can be shown to decay kinematically in an expanding universe and tensor perturbations lead to gravitational waves that do not couple to energy density and pressure inhomogeneities [24]. Any scalar perturbation can be decomposed in terms of eigenmodes of the laplacian on the constant  $\eta$  surface:

$$\nabla^2 Q \equiv \gamma^{ij} Q_{|ij} = -k^2 Y \quad (7)$$

where '|' represents a covariant derivative with respect to the three metric  $\gamma_{ij}$ . The most general form for the line element with scalar metric perturbations in the longitudinal gauge is (see eg. [25, 26])

$$ds^2 = a^2(\eta)[(1 + 2\Phi)d\eta^2 - (1 - \Psi)\gamma_{ij}dx^i dx^j] \quad (8)$$

Similarly, perturbations of the stress tensor can be described in terms of velocity and density perturbations in the longitudinal gauge ( $v^{(long)}$ ,  $\delta^{(long)}$ ). We define the matter gauge invariant variables as usual [26] (the dot “.” is a derivative with respect to  $\eta$ ):

$$V \equiv v^{(long)} \quad (9)$$

$$D_g \equiv \delta^{(long)} + 3(1+w)\Phi, \quad w \equiv p/\rho \quad (10)$$

$$D \equiv \delta^{(long)} + 3(1+w)\frac{\dot{a}}{a}\frac{V}{k} \quad (11)$$

For a perfect fluid,  $\Phi = -\Psi$  and the full compliment of scalar perturbation equations read:

$$4\pi G a^2 \rho D = (k^2 + 3)\Phi \quad (12)$$

$$4\pi G a^2 (\rho + p)V = k\left(\frac{\dot{a}}{a}\Psi - \dot{\Phi}\right) \quad (13)$$

$$\dot{D}_g + 3(c_s^2 - w)D_g \dot{a}/a + (1+w)kV + 3w\Gamma \dot{a}/a = 0 \quad (14)$$

$$\dot{V} + (1 - 3c_s^2)V\frac{\dot{a}}{a} = k(\Psi - 3c_s^2\Phi) + \frac{c_s^2 k}{1+w}D_g + \frac{wk}{1+w}\Gamma \quad (15)$$

where  $c_s$  is the sound speed and  $\Gamma \equiv \Pi_l - c_s^2\delta/w$  vanishes for adiabatic perturbations (see eg. [26, 25]). For pure dust  $w = c_s^2 = p = 0$  and the above equations reduce to:

$$\dot{D}_g + kV = 0 \quad (16)$$

$$\dot{V} + V\frac{\dot{a}}{a} = k\Psi \quad (17)$$

$$-k^2\Psi = 4\pi G a^2 \rho (D_g + 3(\Psi + \frac{\dot{a}}{a}\frac{V}{k})) \quad (18)$$

In terms of the present density,

$$C \equiv 4\pi G \rho_o a_0^2 = \frac{3}{2} \frac{8\pi G}{3H_o^2} \rho_o = \frac{3}{2} \Omega_b \approx 0.3 \quad \text{for } \Omega_b \approx 0.2$$

the density perturbation equation simply reduces to:

$$[(k^2 + 3)\frac{e^\eta}{C} + 3]\ddot{D}_g + [(k^2 + 3)\frac{e^\eta}{C} + 2]\dot{D}_g - D_g k^2 = 0 \quad (19)$$



$k = 1$  corresponds to the Hubble scale which is the same as the curvature scale in this model. At a redshift  $\approx 1000$ , this scale subtends an angle roughly .25 degrees. Using constraints from microwave background anisotropy at these angles gives  $D_g \approx 10^{-5}$  at these scales at the last scattering surface. It is easy to see that modes  $k \lesssim 1$  do not grow. At smaller angular scales (large  $k$ ), the observed anisotropy is expected to fall to much lower values [27]. Diffusion damping dampens anisotropies at angular scales smaller than about one minute. However, for such large values of  $k$ ,  $D_g$  has rapidly growing solutions. Eqn.(19) goes as

$$\ddot{D}_g + \dot{D}_g - Ce^{-\eta}D_g = 0 \quad (20)$$

This has exact solutions in terms of modified first and second type bessel functions  $I_1$ ,  $K_1$ :

$$D_g = C_1(Ce^{-\eta})^{\frac{1}{2}}I_1((4Ce^{-\eta})^{\frac{1}{2}}) + C_2(Ce^{-\eta})^{\frac{1}{2}}K_1((4Ce^{-\eta})^{\frac{1}{2}}) \quad (21)$$

For large arguments, these functions have their asymptotic forms:

$$I_1 \longrightarrow \frac{(Ce^{-\eta})^{-\frac{1}{4}}}{2\sqrt{\pi}}exp[2(Ce^{-\eta})^{\frac{1}{2}}]; \quad K_1 \longrightarrow \frac{(Ce^{-\eta})^{-\frac{1}{4}}}{2\sqrt{\pi}}exp[-2(Ce^{-\eta})^{\frac{1}{2}}] \quad (22)$$

Even if diffusion damping were to reduce the baryon density contrast to values as low as some  $10^{-15}$ , a straight forward numerical integration of eqn(19) demonstrates that for  $k \geq 3000$  the density contrast becomes non linear around redshift of the order 50.

In contrast to the above, in the radiation dominated epoch  $w = c_s^2 = 1/3$ . In adiabatic approximation, eqns(12,15) imply:

$$[(k^2 + 3)\frac{3}{4k^2} + \frac{3\tilde{C}}{2k^2e^{2\eta}}]\ddot{D}_g + \frac{3\tilde{C}}{k^2e^{2\eta}}\dot{D}_g + [\frac{k^2 + 3}{8} - \frac{\tilde{C}}{2e^{2\eta}}]D_g = 0 \quad (23)$$

For  $\eta$  large and negative, small  $k$  perturbation equation reduces to

$$3\ddot{D}_g + 6\dot{D}_g - k^2D_g = 0 \quad (24)$$

It is straightforward to demonstrate that perturbations bounded for large negative  $\eta$ , damp out for small  $k$ . It is more instructive to work with the equation for the potential for large  $k$  perturbations:

$$\ddot{\Phi} + 3(1 + c_s^2)\dot{\Phi} + [2(1 + 3c_s^2) + k^2c_s^2]\Phi = 0 \quad (25)$$

when

$$\delta^{long} = \frac{2e^{2\eta}}{3\Omega_\gamma} [3\dot{\Phi} + k^2\Phi] \quad (26)$$

For  $c_s = 1/3$ , the solutions are

$$\Phi \propto e^{-2\eta} e^{\pm(\frac{ik\eta}{\sqrt{3}})} \quad (27)$$

$$\delta^{long} \propto (k^2 \pm \sqrt{3}ik) e^{\pm(\frac{ik\eta}{\sqrt{3}})} \quad (28)$$

Thus we get oscillating solutions for the potential as well as the density fluctuations. These fluctuations shall manifest themselves as ‘‘acoustic’’ fluctuations in the Cosmic microwave background sky to which we shall return later.

We summarize here by noting that fluctuations do not grow in the radiation dominated era, small  $k$  (large scale) fluctuations do not grow in the matter dominated era as well, however, even tiny residual fluctuations  $O(10^{-15})$  at the last scattering surface for large values of  $k \geq 3000$  in the matter dominated era, can in principle grow to the non linear regime. Such a growth would be a necessary condition for structure formation and is not satisfied in the standard model. In the standard model, cold dark matter is absolutely essential for growth. Thus a linear coasting model does not need such dark matter to have small density perturbations approach a non linear regime necessary for a structure formation theory.

### c) The recombination epoch

Salient features of the plasma era in a linear coasting cosmology have been described in [28, 27]. Here we reproduce some of the peculiarities at the recombination epoch. These are deduced by making a simplifying assumption of thermodynamic equilibrium just before recombination.

A recombination process that directly produces a Hydrogen atom in the ground state releases a photon with energy  $B = 13.6eV$  in each recombination.  $n_\gamma(B)$ , the number density of photons in the background radiation with energy  $B$ , is given by [see eg. [29]]:

$$\frac{n_\gamma(B)}{n} = \frac{16\pi}{n} T^3 \exp\left(\frac{-B}{T}\right) \approx \frac{2 \times 10^6}{h^2} \exp\left(\frac{-13.6}{\tau}\right) \quad (29)$$

Where  $\tau$  is the temperature in units of eV. This ratio is unity at  $\tau \approx .9$  for  $\Omega_B h^2 \approx 1$  and decreases rapidly at lower temperatures. Any 13.6 eV photons released due to recombination have a high probability of ionizing neutral atoms formed a little earlier. This process is therefore not very effective for producing a net number of neutral atoms. The way out of this impasse is the *two photon emission*. The  $2S \rightarrow 1S$  transition is strictly forbidden at first order. The conservation of both the energy and angular momentum in the transition can take place only by emission of a pair of photons. This gives a mechanism for transferring the ionization energy into photons with  $\lambda > \lambda_{Ly\alpha}$ . Since the reverse process does not occur at the same rate, this is non-equilibrium recombination. Being a process of second order in perturbation theory, this is slow (lifetime  $\approx 0.1$  sec). As recombination has to pass through this bottleneck, it proceeds with a rate different from the Saha prediction.

In the red-shift range  $800 < z < 1200$ , the approximate fractional ionization in a linearly coasting cosmology can be approximated by [27]:

$$x_e = \frac{7.6 \times 10^{-5}}{\Omega_b h} \left(\frac{z}{1000}\right)^{12.25} \quad (30)$$

The optical depth for Thompson scattering is then:

$$\tau_\gamma = \int_0^t n_B(t) x_e(t) \sigma_T dt = - \int_0^z n_B(z) x_e(z) \sigma_T \left(\frac{dt}{dz}\right) dz \quad (31)$$

With  $n_b(z) = \eta n_\gamma(z) = \eta \times 421.8(1+z)^3 \text{ cm}^{-3}$ , and

$$\frac{dt}{dz} = -\frac{1}{H_0(1+z)^2} \quad (32)$$

one can find the red-shift at which the optical depth goes to unity. With the residual ionization  $x_{e,res}$ , we get

$$\tau_\gamma = 0.55 \left(\frac{z}{1000}\right)^{14.25} \quad (33)$$

From this optical depth, we can compute the probability that a photon was last scattered in the interval  $(z, z + dz)$ . This is given by:

$$P(z) = e^{-\tau_\gamma} \frac{d\tau_\gamma}{dz} \approx 7.85 \times 10^{-3} \left(\frac{z}{1000}\right)^{13.25} \exp\left[-0.55 \left(\frac{z}{1000}\right)^{14.25}\right] \quad (34)$$

This  $P(z)$  is sharply peaked and well fitted by a gaussian of mean redshift  $z \approx 1037$  and standard deviation in redshift  $\Delta z \approx 67.88$ . Thus in a linearly coasting cosmology, the last scattering surface locates at redshift  $z^* = 1037$  with thickness  $\Delta z \approx 68$ . Corresponding values in standard cosmology are  $z = 1065$  and  $\Delta z \approx 80$  [30].

An important scale that determines the nature of CMBR anisotropy is the Hubble scale which is the same as the curvature scale for linear coasting. The angle subtended today, by the Hubble radius at  $z^* = 1037$ , is determined by the angular diameter - redshift relation:

$$r_R \sin \frac{\theta}{2} = \sinh \left[ \frac{d(\theta)(1+z_R)}{2a_o} \right] \quad (35)$$

For  $d(\theta) = 2d_H(t_R) = 2H(t_R)^{-1} = 2[H_o(1+z_R)]^{-1}$  and  $r_R \approx (1+z)/2$ , this gives:

$$\left( \frac{1+z_R}{2} \right) \frac{\theta}{2} = \sinh(1) \quad (36)$$

or  $\theta_H \approx 15.5$  minutes.

In standard cosmology, the *sound horizon* is of the same order as the Hubble length at recombination. The Hubble length determines the scale over which physical processes can occur coherently. Thus, as we suggest in the next section, one expects all acoustic signals to be contained within an angle of the order of the angle subtended by the Hubble length at recombination.

In a linear coasting, the Hubble length is precisely the inverse of the curvature scale. However, the sound horizon ( $s^*$ ) is much larger. Strictly speaking, the particle as well as the sound horizon are infinite for a linear coasting cosmology. As we would see, the CMB anisotropy pattern frozen on the Last scattering surface depends on the distance travelled by pressure waves from the epoch baryon density starts becoming comparable to radiation density. The photon diffusion scale is determined by the thickness of the LSS. With  $z^* \approx 1037$  and  $\Delta z \approx 68$ , the photon diffusion scale projected on the LSS corresponds to an angular size roughly one thirteenth of the Hubble length at the LSS. This subtends an angle of roughly one minute at the current epoch.

The above scales in principle determine the nature of CMB anisotropy. The CMB effectively ceases to scatter when the optical depth to the present drops to unity. After last scattering, the photons effectively free stream. On

the LSS, the photon distribution may be locally isotropic while still possessing inhomogeneities i.e. hot and cold spots, which will be observed as anisotropies in the sky today (see eg. [31, 32]).

#### d) The CMB temperature anisotropy

The fractional temperature fluctuation  $\Theta(t, \mathbf{x}, \gamma)$  for a black body is defined as

$$4\Theta \equiv \frac{\delta\rho_\gamma}{\rho_\gamma} \quad (37)$$

where  $\rho_\gamma \propto T^4$  is the spatially and directionally averaged energy density of the photons.  $\Theta$  satisfies the collisionless Boltzmann equation [31, 27]:

$$\frac{d}{d\eta}[\Theta + \Phi](\eta, \mathbf{x}, \gamma) = \dot{\Phi} + \dot{\Psi} \quad (38)$$

Before recombination photons and baryons were strongly coupled via Compton scattering. In this case the collisional Boltzmann equation is given by

$$\frac{d}{d\eta}(\Theta + \Phi) \equiv \dot{\Theta} + \gamma^i \frac{\partial}{\partial x^i}(\Theta + \Phi) + \dot{\gamma}^i \frac{\partial}{\partial \gamma^i} \Theta - \dot{\Psi} = \dot{\tau}(\Theta_0 - \Theta - \gamma_i v_b^i + \frac{1}{16} \gamma_i \gamma_j \Pi_\gamma^{ij}) \quad (39)$$

where  $\dot{\tau} \equiv x_e n_e \sigma_T$  is the differential optical depth to Thomson scattering with  $\sigma_T = 8\pi\alpha^2/3m_e^2$  as the Thomson scattering Cross-section,  $x_e$  and  $n_e$  are the ionization fraction and total electron density respectively.  $\Theta_0 = \delta_\gamma/4$  is the isotropic component of  $\Theta$ ,  $\gamma^i = \dot{x}^i$ , and the quantities  $\Pi_\gamma^{ij}$  are the quadrupole moments of the energy distribution given by

$$\Pi_\gamma^{ij} = \int \frac{d\Omega}{4\pi} (3\gamma^i \gamma^j - \gamma^{ij}) 4\Theta(\eta, \mathbf{x}, \gamma) \quad (40)$$

Perturbations are expanded in terms of eigenfunctions of the Laplacian. To effect this, spherical coordinates are defined by the the line element

$$dl^2 = \gamma_{ij} dx^i dx^j = -K^{-1} [d\chi^2 + \sinh^2 \chi (d\theta^2 + \sin^2 \theta d\phi^2)] \quad (41)$$

where the distance is scaled to the curvature radius  $\chi = \sqrt{-K}\eta$ . The laplacian of any scalar function  $Q$  is given by:

$$\gamma^{ij} Q_{|ij} = -K \sinh^{-2} \chi \left[ \frac{\partial}{\partial \chi} (\sinh^2 \chi \frac{\partial Q}{\partial \chi}) + \sin^{-1} \theta \frac{\partial}{\partial \theta} (\sin \theta \frac{\partial Q}{\partial \theta}) + \sin^{-2} \theta \frac{\partial^2 Q}{\partial \phi^2} \right] \quad (42)$$

Since the angular part is independent of curvature, we may separate variables such that  $Q = X_\nu^l(\chi)Y_l^m(\theta, \phi)$  and  $\nu^2 \equiv -(k^2/K + 1)$ . The spherically symmetric  $l = 0$  function turns out to be:

$$X_\nu^0(\chi) = \frac{\sin(\nu\chi)}{\nu\sinh\chi} \quad (43)$$

The higher modes are explicitly given by [33]

$$X_\nu^l(\chi) = (-1)^{l+1}M_l^{-1/2}\nu^{-2}(\nu^2 + 1)^{-l/2}\sinh^l\chi\frac{d^{l+1}(\cos\nu\chi)}{d(\cosh\chi)^{l+1}} \quad (44)$$

which reduce to  $j_l(k\eta)$  in the flat space limit, where

$$\begin{aligned} M_l &\equiv \prod_{\nu=0}^l K_\nu \\ K_0 &= 1 \\ K_l &= 1 - (l^2 - 1)K/k^2, \quad l \geq 1. \end{aligned} \quad (45)$$

All these reduce to unity as  $K \rightarrow 0$ . The functions are normalized as [31, 34]

$$\int X_\nu^l(\chi)X_{\nu'}^{l'}(\chi)\sinh^2\chi d\chi = \frac{\pi}{2\nu^2}\delta(\nu - \nu')\delta(l - l') \quad (46)$$

These functions can also be generated from their recursion relations. One particularly useful relation, which is used in the collisionless Boltzmann equation, is [33]

$$\frac{d}{d\eta}X_\nu^l = \frac{l}{2l+1}kK_l^{1/2}X_\nu^{l-1} + \frac{l+1}{2l+1}kK_{l+1}^{1/2}X_\nu^{l+1} \quad (47)$$

Vectors and tensors needed in the description of the velocity and stress perturbations can be constructed from the the covariant derivatives of the scalar function  $Q$  and the metric tensor,

$$\begin{aligned} Q_i &\equiv -k^{-1}Q_{|i} \\ Q_{ij} &\equiv k^{-2}Q_{|ij} + \frac{1}{3}\gamma_{ij}Q \end{aligned} \quad (48)$$

where the indices are to be raised and lowered by the three metric  $\gamma^{ij}$  and  $\gamma_{ij}$ . These vectors and tensors can be used to represent dipoles and quadrupoles,

$G_1 = \gamma^i Q_i$  and  $G_2 = \frac{3}{2} \gamma^i \gamma^j Q_{ij}$ . In general any function of position  $\mathbf{x}$  and angular direction  $\gamma$ , e.g. the radiation distribution function, can be represented as [35]

$$F(\mathbf{x}, \gamma) = \sum_{\tilde{\mathbf{k}}} \sum_{l=0}^{\infty} \tilde{F}_l(\mathbf{k}) G_l(\mathbf{x}, \gamma, \mathbf{k}) \quad (49)$$

where

$$G_l(\mathbf{x}, \gamma, \mathbf{k}) = (-k)^{-l} Q_{|i_1 \dots i_l}(\mathbf{x}, \mathbf{k}) P_l^{i_1 \dots i_l}(\mathbf{x}, \gamma) \quad (50)$$

and  $\tilde{k}^2 = K(k^2/K + 1)$  and

$$\begin{aligned} P_0 &= 1, & P_1^i &= \gamma^i \\ P_2^{ij} &= \frac{1}{2}(3\gamma^i \gamma^j - \gamma^{ij}) \\ P_{l+1}^{i_1 \dots i_l} &= \frac{2l+1}{l+1} \gamma^{(i_1} P_l^{i_2 \dots i_{l+1})} - \frac{l}{l+1} \gamma^{(i_1 i_2} P_{l-1}^{i_3 \dots i_{l+1})} \end{aligned} \quad (51)$$

with parentheses denoting symmetrization about the indices.

The multipole decomposition of  $\Theta$  reads:

$$\Theta(\eta, \mathbf{x}, \gamma) = \sum_{l=0}^{\infty} \Theta_l(\eta) M_l^{-1/2} G_l(\mathbf{x}, \gamma) \quad (52)$$

Recursion relations for  $G_l$  give the standard hierarchy of coupled equations for the  $l$ -modes:

$$\begin{aligned} \dot{\Theta}_0 &= -\frac{k}{3} \Theta_1 + \dot{\Psi}, \\ \dot{\Theta}_1 &= k[\Theta_0 + \Phi - \frac{2}{5} K_2^{1/2} \Theta_2] - \dot{\tau}(\Theta_1 - V_b), \\ \dot{\Theta}_2 &= k[\frac{2}{3} K_2^{1/2} \Theta_1 - \frac{3}{7} K_3^{1/2} \Theta_3] - \frac{9}{10} \dot{\tau} \Theta_2, \\ \dot{\Theta}_l &= k[\frac{l}{2l-1} K_l^{1/2} \Theta_{l-1} - \frac{l+1}{2l+3} K_{l+1}^{1/2} \Theta_{l+1}] - \dot{\tau} \Theta_l, \quad (l > 2) \end{aligned} \quad (53)$$

where  $\gamma_i v_b^i(\mathbf{x}) = V_b G_1(\mathbf{x}, \gamma)$  and  $K_l = 1 - (l^2 - 1)K/k^2$ .

Before recombination, Compton scattering transfers momentum between the photons and baryons. From the conservation of momentum of the photon baryon fluid, we get

$$\dot{\delta}_b = -kV_b + 3\dot{\Psi}$$

$$\dot{V}_b = -\frac{\dot{a}}{a}V_b + k\Phi + \dot{\tau}(V_\gamma - V_b)/R \quad (54)$$

where  $R = 3\rho_b/4\rho_\gamma$ . The baryon continuity equation can also be combined with the photon continuity equation to obtain [31]

$$\dot{\delta}_b = -k(V_b - V_\gamma) + \frac{3}{4}\dot{\delta}_\gamma \quad (55)$$

The differential optical depth  $\dot{\tau}$  is high enough before recombination making Compton scattering extremely rapid and effective. Since photon-baryon tight coupling approximation holds, the Boltzmann eqn(53) and the Euler eqn(54) for baryons can be expanded in the Compton scattering time  $\dot{\tau}^{-1}$ . To zeroth order, we get the tight-coupling identities,

$$\begin{aligned} \dot{\Theta}_0 &= \frac{1}{3}\dot{\delta}_b \\ \Theta_1 &\equiv V_\gamma = V_b \\ \Theta_l &= 0 \quad l \geq 2 \end{aligned} \quad (56)$$

These equations merely express the fact that the radiation is isotropic in the baryon rest frame and the density fluctuations in the photons grow adiabatically with the baryons. Substituting the zeroth order solutions back into equations (53) and (54), we obtain the iterative first order equations:

$$\begin{aligned} \dot{\Theta}_0 &= -\frac{k}{3}\Theta_1 + \dot{\Psi} \\ \dot{\Theta}_1 &= -\frac{\dot{R}}{1+R}\Theta_1 + \frac{1}{1+R}k\Theta_0 + k\Phi \end{aligned} \quad (57)$$

where we have used the relation  $\dot{R} = (\dot{a}/a)R$ . The tight coupling approximation eliminates the multiple time scales and the infinite hierarchy of coupled equations of the full problem. These equations can be combined to form a single second order equation,

$$\ddot{\Theta}_0 + \frac{\dot{R}}{1+R}\dot{\Theta}_0 + k^2c_s^2\Theta_0 = F \quad (58)$$



where the photon-baryon sound speed is

$$c_s^2 \equiv \frac{\dot{p}_\gamma}{\dot{\rho}_\gamma + \dot{\rho}_b} = \frac{1}{3} \frac{1}{1+R} \quad (59)$$

assuming that  $p_b \approx 0$  and

$$F = \ddot{\Psi} + \frac{\dot{R}}{1+R} \dot{\Psi} - \frac{k^2}{3} \Phi \quad (60)$$

is the forcing function.

Essential features of CMB anisotropy follow from the above analysis. In the rest of this article we shall be content with making rough estimates of CMB anisotropy peak locations to judge whether there is any a-priori discordance with observations.

Let us first consider ignoring the time dependence of the potentials  $\Psi$  and  $\Phi$  and also the baryon- photon momentum ratio  $R$ . Then eqn(58) reduces to:

$$\ddot{\Theta}_0 + k^2 c_s^2 \Theta_0 = -\frac{k^2}{3} \Phi \quad (61)$$

This is a simple harmonic oscillator under the constant acceleration provided by gravitational infall and its solution is:

$$\Theta_0(\eta) = [\Theta_0(0) + (1+R)\Phi] \cos(kr_s) + \frac{1}{kc_s} \dot{\Theta}_0(0) \sin(kr_s) - (1+R)\Phi \quad (62)$$

where  $r_s$  is the sound horizon given as

$$r_s = \int_{\eta_0}^{\eta} c_s d\eta' \quad (63)$$

where  $\eta_0$  is the epoch of birth of pressure waves. We may take this to be the QGP phase transition epoch  $T_{QGP} \approx 10^{12} K$ , or even earlier. The following results are independent of this initial epoch (cut-off). The distance a sound wave travels from the initial epoch till the epoch  $\eta$  is  $r_s$ .  $\Theta_0(0)$  and  $\dot{\Theta}_0(0)$  govern the form of the acoustic oscillations and govern the adiabatic and isocurvature modes respectively. Eqn(62) also implies, through the photon continuity eqn(57), that

$$\Theta_1(\eta) = 3[\Theta_0(0) + (1+R)\Phi] c_s \sin(kr_s) + 3 \frac{1}{k} \dot{\Theta}_0(0) \cos(kr_s) \quad (64)$$

In eqns(62, 64) lie the main acoustic and redshift effects which dominate primary anisotropy formation. In the early universe, photons dominate the fluid and  $R \rightarrow 0$ . In this limit, the oscillation takes on an even simpler form. For the adiabatic mode,  $\dot{\Theta}_0(0) = 0$  and  $\Theta_0(\eta) = [\Theta_0(0) + \Phi]\cos(kr_s) - \Phi$ . This represents an oscillator with a zero point which has been displaced by gravity. The zero point represents the state at which gravity and pressure are balanced. The displacement  $-\Phi > 0$  yields hotter photons in the potential well since gravitational infall not only increases the number density of the photons but also their energy through gravitational blueshifts.

However, photons also suffer a gravitational redshift from climbing out of the potential well after last scattering. This precisely cancels the  $-\Phi$  blueshift. Thus the effective temperature perturbation is  $\Theta_0(\eta) + \Phi = [\Theta_0(0) + \Phi]\cos(kr_s)$ . This takes care of two sources of primary anisotropy: gravity and intrinsic temperature variations on the last scattering surface. The final source in this (tight coupling) approximation is the Doppler shift. The bulk velocity of the fluid along the line of sight is  $V_\gamma/\sqrt{3} = \Theta_1/\sqrt{3}$ . This causes the observed temperature to be Doppler shifted. Eqn(64) shows that the acoustic velocity  $\Theta_1$  is  $\pi/2$  out of phase with the temperature. Because of its phase relation, the velocity contribution fills in the zeros of the temperature oscillations. The rms temperature fluctuation is identically smoothed out leaving no residual primary anisotropies.

This null result gets altered once we take into account of a non-vanishing  $R$ . Baryons add gravitational and inertial mass to the fluid,  $m_{eff} = 1 + R$ , without affecting the pressure. This decreases the sound speed and changes the balance of pressure and gravity. Gravitational infall now leads to greater compression of the fluid in a potential well, i.e. a further displacement of the oscillation zero point. Since the redshift is not affected by the baryon content, this relative shift remains after last scattering to enhance all peaks from compression over those from rarefaction. To demonstrate the effect of  $R \neq 0$ , let us assume it to be constant and non-vanishing after an epoch  $\eta = \eta_1$  and negligible earlier. For an adiabatic perturbation,  $\dot{\Theta}_0(0) = 0$  we have:

$$\Theta(\eta_1) = [\Theta(0) + \Phi]\cos\left(\frac{k}{\sqrt{3}}\eta_1\right) - \Phi \quad (65)$$

$$\dot{\Theta}(\eta_1) = -\frac{k}{\sqrt{3}}[\Theta(0) + \Phi]\sin\left(\frac{k}{\sqrt{3}}\eta_1\right) \quad (66)$$

Thus after  $\eta = \eta_1$ , the solution reads:

$$\begin{aligned} \Theta(\eta) + (1 + R)\Phi &= [\Theta(0) + \Phi] \left[ \cos\left(\frac{k}{\sqrt{3}}\eta_1\right) \cos\left(\frac{k}{\sqrt{3(1+R)}}(\eta - \eta_1)\right) \right. \\ &\quad \left. - \sqrt{1+R} \sin\left(\frac{k}{\sqrt{3}}\eta_1\right) \sin\left(\frac{k}{\sqrt{3(1+R)}}(\eta - \eta_1)\right) \right] + R\Phi \cos\left(\frac{k}{\sqrt{3(1+R)}}(\eta - \eta_1)\right) \end{aligned} \quad (67)$$

The phase of the oscillation freezes at the last scattering surface  $\eta = \eta^*$  and determines the observed fluctuation pattern. For a linear coasting cosmology,  $|\eta_1|$  is large. It is in fact infinite for a universe starting at  $t = 0$ , and can be made finite (but large) only by choosing a lower cutoff for  $t$ . The angular power spectrum of the above expression is obtained by transforming it with respect to the ultraspherical bessel functions [31, 34]. A given  $k$  mode would contribute to two distinct angular scales: (1) A very small angular scale corresponding to the large phase of the first two harmonic functions, and (2) the angular scale corresponding to the third harmonic function:

$$+R\Phi \cos\left(\frac{k}{\sqrt{3(1+R)}}(\eta^* - \eta_1)\right)$$

For  $\Omega_b \approx 0.2$  and  $h \approx 0.7$ , significant deviation of  $c_s$  from  $1/\sqrt{3}$  occur around the matter radiation equality at redshift given by  $1 + z_{eq} \approx 3.9 \times 10^4 (\Omega_b h^2) \approx 4000$ . Thus only those fluctuations that originate at redshift  $\tilde{z} = \text{few} \times z_{eq}$  would give rise to observable temperature anisotropies at LSS which locates at  $z^* \approx 1037$ . The argument of the above harmonic pattern freezes at LSS and would give rise to “peaks” at

$$\frac{k}{\sqrt{3(1+R)}} a_{Rec} \ln\left(\frac{\tilde{z}}{z_r}\right) = n\pi \quad (68)$$

The corresponding wavelengths are at

$$\lambda_n^a = \frac{\pi}{k_n} \quad (69)$$

The first “peak” is at  $k_a = 0$  and the second at roughly  $\theta \approx 15$  minutes. Compression peaks occur at odd values of  $n$  and are located at angles  $\theta_n^a =$

$15/n\pi$  minutes. The entire analysis can be repeated for isocurvature modes to find the peaks located at even  $n$  at  $\theta_n^i = 15/(n + \frac{1}{2})$  minutes.

The above analysis has not taken into account the variation of  $R$ . For a qualitative comparison one has to integrate eqn(58). Using a WKB approximation (which is good for modes for which the time scale of variation of sound speed is greater than the oscillation period) it can be seen [31] that the phase structure only suffers a minor change from the above analysis while most of the effect of changing  $R$  effects the amplitude of the solution.

The exact profile of the anisotropy would be determined by the choice of the nature of initial conditions (adiabatic or isocurvature), the chosen initial power spectrum, and the growth of perturbations after  $z^*$  (these determine the late or the *integrated SW effect*), aspects of reionization etc. As photons possess a mean free path in the Baryons  $\lambda_c \approx \dot{\tau}^{-1}$  due to Compton scattering, the photon-baryon tight coupling breaks down at the photon diffusion scale. Finally, after last scattering, photons free stream toward the observer on radial null geodesics and suffer only the gravitational interactions of redshift and dilation. Spatial fluctuations on the last scattering surface are observed as anisotropies in the sky. Free streaming thus transfers  $l = 0$  inhomogeneities and  $l = 1$  bulk velocities to high multipoles as the  $l$ -mode coupling of the Boltzmann eqn(53) suggests. Isotropic  $l = 0$  density perturbations are thus averaged away collisionlessly.

### 3 Summary

The main point we make in this article is that in spite of a significantly different evolution, the recombination history of a linearly coasting cosmology can be expected to give the location of the primary acoustic peaks in the same range of angles as that given in Standard Cosmology. Given that none of the alternative anisotropy formation scenarios provide a compelling *ab initio* model [39], it is perhaps best to keep an open mind to all possibilities. As the large scale structure and CMB anisotropy data continue to accumulate, one could explore the general principles for an open coasting cosmology to aid in the empirical reconstruction of a consistent model for structure formation.

Finally, we are tempted to mention that a linear coasting cosmology presents itself as a falsifiable model. It is encouraging to observe its concordance !! In standard cosmology, falsifiability has taken on a backstage - one just constrains the values of cosmological parameters subjecting the data to Bayesian statistics. Ideally, one would have been very content with a cosmology based on physics that we have already tested in the laboratory. Clearly, standard cosmology does not pass that test. One needs a mixture of hot and cold dark matter, together with (now) some form of *dark energy* to act as a cosmological constant, to find any concordance with observations. In other words, one uses observations to parametrize theory in Standard Cosmology.

Linear coasting presents a very distinguishable cosmology. Recombination occurs at age  $\sim 10^7$  years as opposed to  $\sim 10^5$  years in standard cosmology. The Hubble scale at decoupling is thus two orders of magnitude greater in linear coasting. This fact, coupled with the absence of any horizon, could well have falsified linear coasting. Any concordance with observations is therefore very significant. The model comes with its characteristic predictions. Thus linear coasting has the potential of relegating the need for any form of dark matter or dark energy (or for that matter, any physics not already tested in the laboratory) to the physics archives where they enjoy the same status as ether and phlogiston. The message this article is to convey is that a universe that is born and evolves as a curvature dominated model has a tremendous concordance and there are sufficient grounds to explore models that support such a coasting.

## Acknowledgments

We thank the University Grants Commission for financial support. The work benefited from discussions with Profs. T. Padmanabhan, K. Subrahmanian and T. Saurodeep and the same are gratefully acknowledged.

## References

- [1] D.Lohiya, A. Batra, M. Sethi, *Phys. Rev.* **D60**, 108301 (2000); M. Sethi & D. Lohiya, *Class. Quant. Grav* **16**, 1 (1999); *Grav. & Cosm* **6**, 1 (1999); A. Dev et al, *Phys. Lett* **B504**, 207 (2001); *Phys. Lett* **B548**, 12 (2002); A. Batra et al, *Int. J. Mod. Phys* **D9**, 757 (2000)
- [2] G. F. R. Ellis, *Gen. Rel. & Grav.* **32**, 1135 (2000)
- [3] J. Ehlers, *Gen. Rel. & Grav.* **25**, 1225 (1993)
- [4] R. Tavakol and R. Zalaletdinov, *gr-qc/9703025; gr-qc/9703016*
- [5] E. A. Milne, “Relativity Gravitation and World Structure”, Oxford (1935); “Kinematic Relativity”, Oxford (1948)
- [6] W. Rindler, “Essential Relativity”, Van Norstrand, (1965)
- [7] A. D. Dolgov in the *The Very Early Universe*, eds. G. Gibbons, S. Siklos, S. W. Hawking, C. U. Press, (1982); *Phys. Rev.* **D55**,5881 (1997).
- [8] S. Weinberg, *Rev. Mod. Phys.* **61**, 1 (1989)
- [9] L.H. Ford, *Phys Rev* **D35**,2339 (1987).
- [10] R.E.Allen *astro-ph/9902042*.
- [11] P.Manheim & D.Kazanas, *Gen. Rel. & Grav.* **22**,289 (1990).
- [12] E. W. Kolb, *ApJ* **344**, 543 (1989)
- [13] S.Perlmutter, et al., *astro-ph/9812133; Nature* **391**, 51 (1998); *ApJ* **483**, 565 (1997).

- [14] W.L. Freedman, J.R. Mould, R.C. Kennicutt, & B.F. Madore, *astro-ph/9801080*.
- [15] D.Branch, *Ann.Rev.of Astronomy and Astrophysics* **36**, 17 (1998), *astro-ph/9801065*.
- [16] M.Hamuy, et al., *Astron. J.* **112**, 2391 (1996).
- [17] M.Hamuy et al., *Astron. J.* **109**, 1 (1995).
- [18] Kaplinghat, G. Steigman et. al. *Phys. Rev.* **D59**, 043514 (1999).
- [19] Epstein, R.I., Lattimer, J.M., and Schramm, D.N. *Nature* **263**, 198 (1976).
- [20] R. B. Tully and E. J. Shaya, “Proceedings: Evolution of large scale structure” - Garching, (1998)
- [21] P. J. E. Peebles, “Principles of Physical Cosmology” Princeton University Press, Princeton, (1993)
- [22] E. Bertschinger, *astro-ph/9503125*; *Cosmological Dynamics*, Elsevier Science Publishers (1999)
- [23] G. W. Gibbons, Private notes on Central Configurations
- [24] J. Bardeen, *Phys. Rev.* **D22**, 1882 (1980)
- [25] V. F. Mukhanov, H. A. Feldman and R. H. Brandenberger, *Phys. Rep.* **215** 203 (1992)
- [26] Ruth Durrer, *astro-ph/0109522* (2001).
- [27] Savita Gehlaut, “A Concordant Linear Coasting Cosmology” PhD thesis, University of Delhi, (2003).
- [28] S. Gehlaut, A. Mukherjee, S. Mahajan, D. Lohiya, “A freely Coasting Universe”, *Spacetime and Substance* **4**, 14 (2002)
- [29] S. Seager, D. D. Sasselov, D. Scott, *ApJ* **523**: L1-L5 (1999).

- [30] T. Padmanabhan, “Structure formation in the Universe”, Cambridge University Press (1993)
- [31] Wayne Hu, PhD thesis, Berkeley (1995) and references therein.
- [32] M. Tegmark, *astro-ph/9511148* 1995
- [33] L. F. Abbot and R. K. Schaefer, *ApJ.* **308**, 546 (1986)
- [34] D. H. Lyth and A. Woszczyna, *Phys. Rev.* **D51**, 2599 (1995)
- [35] M. L. Wilson, *ApJ.* **273**, 2 (1983)
- [36] W. Hu and N. Sugiyama, *Phys. Rev.* **D51**, 2599 (1995)
- [37] W. Hu and N. Sugiyama, *ApJ.* **444**, 489 (1995)
- [38] J. Silk, *ApJ.* **151**, 459 (1969)
- [39] W. Hu *astro-ph/95111130*



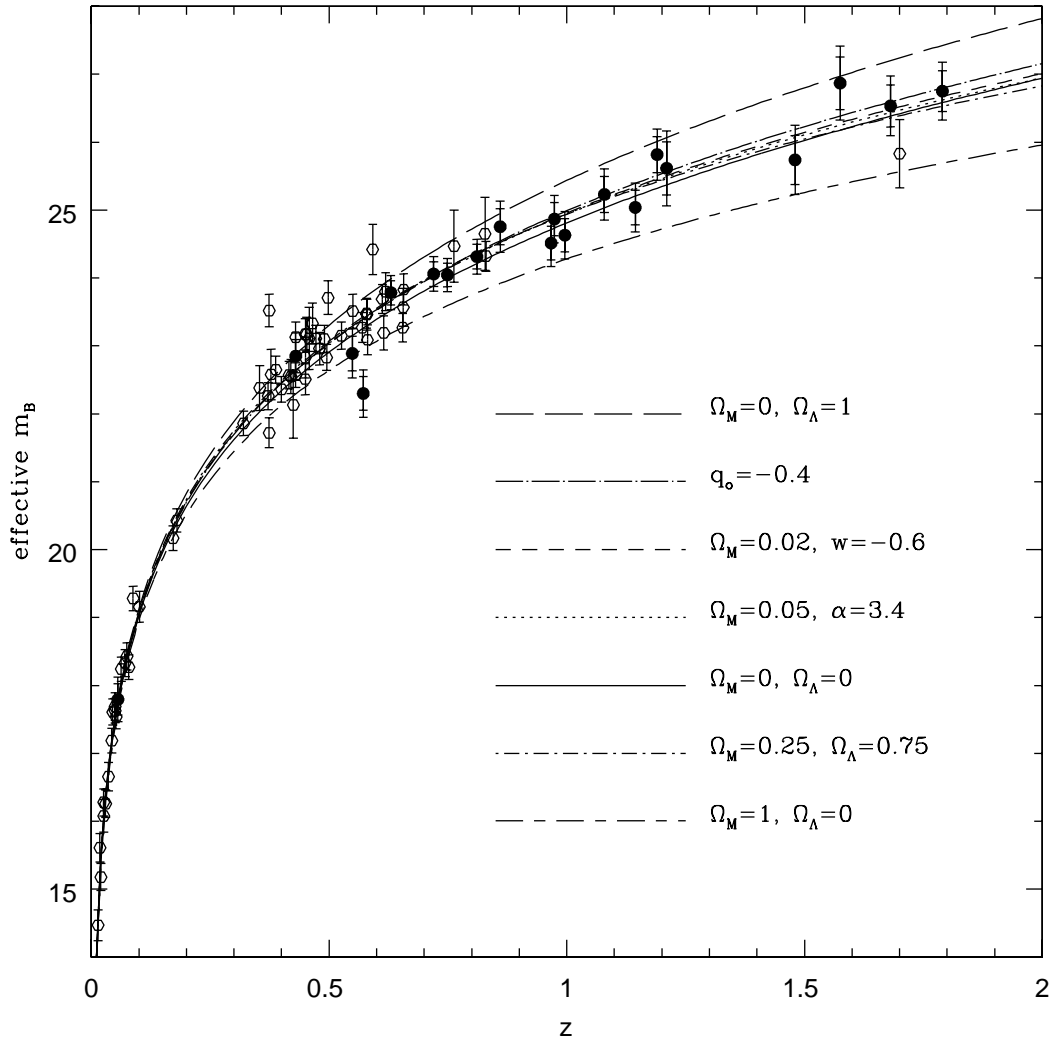


Figure 1: Hubble diagram, taken from the supernova cosmology project. “The curve for  $(\Omega_\Lambda, \Omega_M) = (0, 0)$  is practically identical to the best fit unconstrained cosmology” [13].